Earth Syst. Dynam. Discuss., doi:10.5194/esd-2017-11, 2017
Manuscript under review for journal Earth Syst. Dynam.
Published: 7 February 2017

Earth System Dynamics
Discussions
Open Access
EGU

Emission metrics for quantifying regional climate impacts of aviation

Marianne T. Lund[*,1], *Borgar Aamaas*[1], *Terje Berntsen*[1,2], *Lisa Bock*[3], *Ulrike Burkhardt*[3], *Jan S. Fuglestvedt*[1], *Keith P. Shine*[4]

1 CICERO, Center for International Climate and Environmental Research Oslo, Norway

2 Department of Geosciences, University of Oslo, Norway

3 Deutsches Zentrum für Luft- und Raumfahrt, Institut für Physik der Atmosphäre, Oberpfaffenhofen, Germany

4 Department of Meteorology, University of Reading, UK

Earth Syst. Dynam. Discuss., doi:10.5194/esd-2017-11, 2017
Manuscript under review for journal Earth Syst. Dynam.
Published: 7 February 2017

Earth System Dynamics
Discussions
Open Access
EGU

ABSTRACT

This study examines the impacts of emissions from aviation in six source regions on global and regional temperature. We consider the NOx-induced impacts on ozone and methane, aerosols and contrail-cirrus formation, and calculate the global and regional climate metrics Global Warming Potential (GWP), Global Temperature change Potential (GTP) and Absolute Regional Temperature change Potential (ARTP). GWPs and GTPs vary by a factor 2-4 between source regions. We find the highest aviation aerosol metric values for South Asian emissions, while contrail-cirrus metrics are higher for Europe and North America, where contrail formation is prevalent, and South America plus Africa, where the optical depth is large once contrails form. The ARTP illustrate important differences in the latitudinal patterns of radiative forcing (RF) and temperature response: The temperature response in a given latitude band can be considerably stronger than suggested by the RF in that band, also emphasizing the importance of large-scale circulation impacts. To place our metrics in context, we quantify the temperature response in the four broad latitude bands following a one-year pulse emission from present-day aviation, including CO_2. Aviation over North America and Europe cause the largest net warming impact in all latitude bands, reflecting the higher air traffic activity here. For all regions, the largest single warming contribution is from contrail-cirrus 20 years after the emissions, while CO_2 becomes dominant at 100 years, although contrail-cirrus remain important in several regions also on this time scale. Our emission metrics can be further used to estimate regional temperature impact under alternative aviation emission scenarios. A first evaluation of the ARTP in the context of aviation suggests that further work to account for vertical sensitivities in the relationship between RF and temperature response would be valuable for further use of the concept.

Earth Syst. Dynam. Discuss., doi:10.5194/esd-2017-11, 2017
Manuscript under review for journal Earth Syst. Dynam.
Published: 7 February 2017

Earth System Dynamics Discussions
Open Access
EGU

1 Introduction

The global aviation sector has historically been one of most rapidly growing economic sectors, and the increase in activity is projected to continue in the foreseeable future. The impacts of aviation exhaust emissions on atmosphere and climate have been under scrutiny for several decades (e.g., (Brasseur et al., 2016; Fahey et al., 1995; Lee et al., 2009; Penner et al., 1999; Sausen et al., 2005). Today, global aviation contributes about 2% of the total anthropogenic CO_2 emissions. In addition to emissions of CO_2, aviation impacts climate through a number of other mechanisms, including emissions of nitrogen oxides (NOx), aerosols and precursor species, aerosol-cloud interactions and formation of contrail-cirrus. These have a much shorter lifetime than a perturbation to CO_2 and hence produce distinctly inhomogeneous radiative forcing and contribute to further inhomogeneity in temperature response. Moreover, the regional and global climate impact of equal emissions of short-lived species can vary depending on where, and even when, the emissions occur. Knowledge of such regional and temporal variability is important for understanding the climate impacts of the sector and can be an important consideration in mitigation.

The spatial variability – from emissions through impacts on atmosphere and radiative forcing, to temperature response – that characterizes the aviation sector is well recognized in the scientific community. Several studies have explored the regional differences in aviation NO_x-induced ozone changes and quantified the radiative forcing (RF) of aviation emissions (Gilmore et al., 2013; Köhler et al., 2013; Lee et al., 2009; Olsen et al., 2013; Penner et al., 1999; Sausen et al., 2005; Stevenson & Derwent, 2009; Unger et al., 2013). However, fewer estimates of regional temperature response exist (Huszar et al., 2013; Jacobson et al., 2012; Olivié et al., 2012). Because of the lack of a one-to-one relationship between forcing and response patterns (Boer & Yu, 2003; Shindell et al., 2010), the strength of regional aviation-induced temperature changes cannot be inferred directly from the corresponding RF distributions. The only tools to provide temperature response and other climate variables on a grid point level are comprehensive climate or earth system models. However, most, if not all, individual economic sectors or individual mitigation measures cause small perturbations, making it difficult (or costly) to capture a robust signal of the consequent response in climate models without significantly scaling up the emissions. On the other hand, providing first-order estimates of contributions of individual sectors to total climate impact

Earth Syst. Dynam. Discuss., doi:10.5194/esd-2017-11, 2017
Manuscript under review for journal Earth Syst. Dynam.
Published: 7 February 2017

or of the effects of specific measures is essential for the formulation and assessment of effective mitigation strategies.

Emission metrics, such as the Global Warming Potential (GWP) and Global Temperature change Potential (GTP) are tools which can serve as bridge to policy making, and are commonly used for aggregating information and placing different emissions on a common scale. Several studies have also used simplified climate models to calculate the global mean temperature response to aviation (Berntsen & Fuglestvedt, 2008; Khodayari et al., 2013; Lee et al., 2009; Marais et al., 2008; Skeie et al., 2009). While aggregation and synthesis is often necessary for reasons of applicability, any such spatially aggregated measure has the disadvantage that it hides the underlying spatial distributions of impacts and the strength of regional impacts.

Recent work has advanced the development of metric concepts which can capture regional impacts. Shine et al. (2005a) and Lund et al. (2012) explored the use of non-linear damage functions to capture spatial information about climate impacts in global metrics. Lund et al. (2012) compared the impact of NOx and aerosol emissions from the transport sectors and found that the loss of information due to global averaging was largest in the case of aviation. However, currently the only metric to provide estimates of impacts on a sub-global scale is the Absolute Regional Temperature change Potential (ARTP) (Shindell & Faluvegi, 2009; Shindell & Faluvegi, 2010). The ARTP provides time-varying surface temperature response in four latitude bands to emissions, accounting for the regional RF caused by the emissions. Hence this provides additional insight into the spatial pattern of temperature response to inhomogeneous forcings beyond that available from traditional global metrics. For instance, Collins et al. (2013) used the ARTP from Shindell and Faluvegi (2009) to examine the regional temperature response to emissions of near-term climate forcers in four regions, while Lund et al. (2014) quantified the regional impacts of on-road diesel emissions.

In this study we combine chemistry-transport and radiative transfer modeling to calculate the GWP, GTP and ARTP for aviation emissions. We consider a broad set of forcing mechanisms and emissions in six separate source regions. This allows us to capture *(i)* the impact of regional aviation emissions on global temperature response and *(ii)* the regional temperature response to

Earth Syst. Dynam. Discuss., doi:10.5194/esd-2017-11, 2017
Manuscript under review for journal Earth Syst. Dynam.
Published: 7 February 2017

Earth System Dynamics Discussions
Open Access
EGU

regional emissions. Using the ARTP, we quantify the regional impact of the present-day (i.e., year 2006) aviation sector, showing the contributions over time from individual species and emission regions to the temperature response in different latitude bands. The basis for the ARTP is a set of regional climate sensitivities, derived by a single climate model, expressing the relationship between forcing and subsequent temperature response in the four latitude bands. Taking our analysis one step further, we compare the regional temperature response to aviation ozone and black carbon aerosols estimated using these regional climate sensitivities with results from simulations with three other climate models, hence performing a first evaluation of the application of the ARTP in the context of selected aviation forcing mechanisms.

2 Methodology

2.1 Atmospheric concentrations and radiative forcing

To quantify the changes in atmospheric concentrations of ozone and aerosols resulting from global and regional aviation emissions, the global chemistry-transport model OsloCTM3 is used (Søvde et al., 2012). The model is run with year 2010 meteorology and a T42 resolution (approximately 2.8° x 2.8°) with 60 vertical layers from the surface to 0.1 hPa. Aviation emissions for 2006 are from the AEDT inventory (Wilkerson et al., 2010), while other anthropogenic and biomass burning emissions are from the HTAPv2 (Janssens-Maenhout et al., 2015) and Global Fire Emissions Database version 3 (GFED3; van der Werf et al. (2010)) inventories. A 20% perturbation of aviation emissions of black and organic carbon (BC, OC), sulfured oxide (SO_2) and NOx is applied globally and in six separate emission source regions, covering both hemispheres and the main flight corridors (Fig. 1): North America (NAM), Europe (EUR), East Asia (EAS), South Asia and Middle East (SAS), South America and Africa (SAF) and South Pacific Ocean (SPO). Total aviation emissions in each region is summarized in Table SI1.

For input to the metric calculations (Sect. 2.2), we calculate the global mean RF for each species i and emission region r, as well as the RF averaged over four latitude bands l (90-28°S, 28°S-28°N, 28-60°N and 60-90°N) ($RF_{i,l,r}$). The direct forcing of aviation aerosols is quantified using the 3-dimensional radiative forcing kernels developed by Samset and Myhre (2011), while the NOx-induced ozone forcing is calculated using the Oslo radiative transfer model (RTM), including

Earth Syst. Dynam. Discuss., doi:10.5194/esd-2017-11, 2017
Manuscript under review for journal Earth Syst. Dynam.
Published: 7 February 2017

Earth System Dynamics Discussions

stratospheric temperature adjustment. The Oslo RTM consists of a broad band scheme for longwave radiation and a scheme using the multi-stream DISORT code for shortwave radiation (Myhre et al., 2000). The RF of NOx-induced methane changes is calculated as

$$RF_{CH4,r} = \Delta\tau_{CH4,r} \cdot [CH4]_{2010} \cdot RFeff_{CH4} \cdot f \quad (1)$$

where $\Delta\tau_{CH4,r}$ is the relative change in methane lifetime between the control run and each of the emissions perturbations, $[CH4]_{2010}$ the 2010 global methane concentration of 1788 ppb, $RFeff_{CH4}$ the methane radiative efficiency of 0.36 (mW m^{-2}) ppb^{-1} (IPCC, 2014) and *f* the feedback factor of 1.34 (Holmes et al., 2013). The RF of the subsequent methane-induced O_3 change (O_3LL) (Wild et al., 2001) is calculated as:

$$RF_{O3LL,r} = 0.5 \cdot RF_{CH4} \quad (2)$$

A decrease in atmospheric methane also results in a slight decrease in stratospheric water vapor, and hence an additional small negative impact, included in our RF_{CH4} based on Myhre et al. (2007) as:

$$RF_{SWV,r} = 0.15 \cdot RF_{CH4} \quad (3)$$

To obtain the latitudinal distributions $RF_{CH4,l,r}$ and $RF_{O3LL,l,r}$ we use the same approach as in Collins et al. (2013) and Lund et al. (2014), and scale results according to the latitudinal distribution of methane forcing derived from a global methane concentration perturbation (Fry et al., 2012).

In order to quantify the RF from the formation and persistence of contrail-cirrus caused by global and regional aviation emissions, simulations with ECHAM5-CCMod (Bock & Burkhardt, 2016b; a) are performed at T42 resolution with 41 vertical levels using the same emission inventory and source regions as in the OsloCTM3. ECHAM5-CCMod is based on the ECHAM5-HAM (Lohmann et al., 2008), which is extended by a contrail cirrus scheme with two-moment microphysics. The two-moment microphysical scheme allows for a more realistic representation of the microphysical and optical properties of contrail cirrus. The model is validated and used to provide updated calculations of stratosphere adjusted contrail-cirrus RF by Bock and Burkhardt (2016a), resulting in a global mean RF of 56 mW m^{-2} for the 2006 AEDT aviation emissions used in this study. The existence of contrail-cirrus results in a decrease in natural cirrus clouds, causing a negative RF that partly offsets contrail-cirrus warming. This cooling contribution is not included

Earth Syst. Dynam. Discuss., doi:10.5194/esd-2017-11, 2017
Manuscript under review for journal Earth Syst. Dynam.
Published: 7 February 2017

Earth System Dynamics Discussions
Open Access
EGU

in our analysis, but is estimated to be on the order of 20 percent of the RF of contrail-cirrus on global mean (Burkhardt & Kaercher, 2011).

Resulting RFs by component, source region and latitude band are given in Table SI2. Most of the species have short atmospheric lifetimes and consequently the RF is largest in the latitude bands closest to where the emissions occur. Some contrail-cirrus RF values are negative, which might be due to a change of cloud cover overlap in the model. Our results do not include effects of aerosol cloud interactions. This is an important limitation, as recent studies suggest that indirect effects both via the modification of cirrus clouds and low level clouds could be large (Gettelman & Chen, 2013; Kapadia et al., 2016; Righi et al., 2016; Zhou & Penner, 2014). However, at present uncertainties in these estimates are also very large, and we consider that their inclusion here would be premature. It should be noted that considerable uncertainties in the magnitude of forcing also from other aviation-induced mechanisms remain, and contributes to uncertainties in the emissions metrics.

2.2 Global and regional climate metrics

We present calculations of the global and regional climate metrics GTP, GWP and ARTP for regional aviation emissions. The GWP and GTP methodology is extensively documented in the literature, (e.g., Aamaas et al. (2013); Fuglestvedt et al. (2003); Shine et al. (2005b)). Hence, we only describe the ARTP framework here.

The Absolute Regional Temperature change Potential (ARTP) gives the time-dependent temperature response following a pulse emission in the four latitude bands 90-28°S, 28°S-28°N, 28-60°N and 60-90°N, accounting for the regional RF caused by the emissions. This regional temperature response is calculated using a set of Regional Climate Sensitivities, $RCS_{i,l,m}$. The $RCS_{i,l,m}$ is the unitless regional response in latitude band m due to a radiative forcing in latitude band l caused by a change in species i, relative to global sensitivity. Hence, the $RCS_{i,l,m}$ express the relative regional response pattern. The regional climate sensitivities are developed based on a large set of simulations performed with the coupled atmosphere-ocean climate model GISS (Shindell & Faluvegi, 2009; Shindell & Faluvegi, 2010).

Earth Syst. Dynam. Discuss., doi:10.5194/esd-2017-11, 2017
Manuscript under review for journal Earth Syst. Dynam.
Published: 7 February 2017

Earth System Dynamics Discussions Open Access EGU

For BC, OC, SO_2, NO_x-induced ozone and contrail-cirrus, the ARTP in latitude band *m* at time *H* following a pulse emission (where *H* is significantly longer than the lifetimes/adjustment times of component) is calculated as:

$$ARTP_{i,r,m}(H) = \sum_l \frac{RF_{i,l,r}}{E_{i,r}} \cdot RCS_{i,l,m} \cdot IRF(H) \quad (4)$$

where $RF_{i,l,r}$ is the RF in latitude band *l* caused by one year of emissions $E_{i,r}$ of species *i* in region *r*. The impulse response function IRF(H) is a temporal temperature response to an instantaneous unit pulse of RF, which includes the global climate sensitivity. Here we have used the IRF of Boucher and Reddy (2008), which gives an equilibrium climate sensitivity (ECS) of 1.06 K (W m^{-2})$^{-1}$, equivalent to a 3.9 K equilibrium response to a doubling of CO_2. This is in the upper range reported in the Fifth IPCC Assessment Report (Bindoff et al., 2013). Assuming that the regional climate sensitivities scale linearly with the ECS, adopting a lower value reduces the magnitude of temperature response, and its time evolution, but does not affect the latitudinal distribution.

In the case of NOx-induced methane and subsequent ozone changes, the longer atmospheric residence time demands an additional IRF that describes the atmospheric decay of methane (IRF_{long}). We add:

$$IRF_{long}(t) = e^{-t/\tau} \quad (5)$$

where τ=11.3 years is the adjustment time for methane for this model run. The $ARTP_{long}$ is then calculated following:

$$ARTP_{i,r,m,long}(H) = \sum_l \int_o^t \frac{RF_{l,r}}{E_{i,r}} \cdot IRF_{long}(H-t) \cdot RCS_{i,l,m} \cdot IRF(H-t)dt \quad (6)$$

The net ARTP is the sum of contributions given by Equations 4 and 6.

For OC, sulfate, contrail-cirrus and methane (plus methane-induced ozone changes) we use the $RCS_{i,l,m}$ of the mean of the responses to CO_2 and sulfate, as tabulated in Shindell and Faluvegi (2010). For BC and NOx-induced ozone change the respective $RCS_{i,l,m}$ from Shindell and Faluvegi (2009) (and tabulated in Collins et al. (2013)) are used. For contrail-cirrus, an important caveat is the exclusion of efficacy (i.e., the ratio of the climate sensitivity parameter for a given forcing mechanisms to that of CO_2 changes), which studies indicate could be as low as 0.3-0.6 (Ponater et al., 2005; Rap et al., 2010). While the efficacy is implicitly included in the $RCS_{i,l,m}$ of individual

Earth Syst. Dynam. Discuss., doi:10.5194/esd-2017-11, 2017
Manuscript under review for journal Earth Syst. Dynam.
Published: 7 February 2017

components, to the extent that the driving processes are accounted for the simulations from which the sensitivities are derived, we do not have specific contrail-cirrus $RCS_{i,l,m}$.

Emission metrics are given on a per unit emission basis. However, for contrail-cirrus it is not clear how to pose the metric since no direct correspondence between an emission and the consequent forcing exists in this case. In order to provide consistent mass-based metrics for all components, we adopt the same approach as Fuglestvedt et al. (2010) and calculate the contrail-cirrus GWP, GTP and ARTP per unit CO_2 emitted. However, as also discussed in Fuglestvedt et al. (2010), an alternative is to relate the contrail-cirrus forcing to the distance flown. This approach may be more consistent with the way aircraft generate contrails and here we also provide metrics on a per km basis. Both approaches are problematic when applying the methodology to future air traffic scenario which likely include fuel efficiency improvements. An increase in fuel efficiency causes a higher probability of contrail formation and at the same time a decrease in CO_2 emissions. Therefore, contrail-cirrus RF per CO_2 emission would increase strongly, whereas contrail-cirrus RF per flight distance would increase less so.

In the following, we present emission metrics and calculate temperature changes for time horizons of 20 and 100 years after a one-year pulse of present-day aviation emissions. Real world emissions are of course not pulses, but rather change over time following the development in economic activity, technology and regulations. However, pulse based emission metrics can be used to quantify the net difference between two emission scenarios since any scenario can be viewed as a series of pulse emissions and analyzed through convolution (Eq. 7 below). Metrics for pulse emissions are also useful in themselves for illustrating the temporal behavior of various species. Realistic emissions will be continuous, leading to different relative contributions of short- and long-lived, warming and cooling species over time. Through the use of convolution, our metric framework can be used to estimate the temperature impact following any emission scenarios $E_{i,r}(t)$. For instance, the regional temperature response in latitude band m for species i for a scenario is the convolution of the emission scenario and the ARTP for a pulse emission (Aamaas et al., 2013):

$$\Delta T_{i,r,m}(t) = \int_0^t E_{i,r}(t') \cdot ARTP_{i,r,m}(t - t')dt' \quad (7)$$

For most short-lived species, the result will be a scaling of the ARTP value for a certain time horizon. However, this is not the case for NOx, where the different time scales of the warming

Earth Syst. Dynam. Discuss., doi:10.5194/esd-2017-11, 2017
Manuscript under review for journal Earth Syst. Dynam.
Published: 7 February 2017

ozone effect and cooling effects linked to methane results in a change of the sign of the emission metric over time (as illustrated for GTP by Aamaas et al. (2016)).

2.3 Simulated temperature response

To evaluate the application of the regional climate sensitivities in the context of aviation RF, we compare temperature responses estimated using the ARTP concept with temperature response patterns simulated by three climate models: the NCAR Community Earth System Model (CESM1.2) (Hurrell et al., 2013), HadSM3 (Williams et al., 2001) and ECHAM (Stenke et al., 2008). Simulations with the two latter models were performed within the EU project QUANTIFY (Ponater et al., 2009) and results used in Lund et al. (2012). Simulations with the CESM1.2 are performed for this study using the aviation ozone concentration perturbation from OsloCTM3. In order to obtain a statistically significant response to aviation ozone in the model, the perturbation is scaled by a factor 40 (similar factors were applied in the HadSM3 and ECHAM simulations, see Lund et al. (2012) for details). We run a four member ensemble of 60 years, using the last 30 in the analysis. The statistical significance is assessed using the False Discovery Rate approach (FDR) (Wilks, 2006). Here we focus on regional patterns of temperature response, but we recognize the potential non-linearities that may arise when scaling of this magnitude is applied (e.g., Shine et al. (2012)) and caution that the magnitude of temperature responses should be interpreted with care. Figure SI 1A) shows the zonal mean aviation-induced ozone concentration from the OsloCTM3 used in simulations with the CESM1.2 and Fig. SI 1B) shows the annual mean temperature response to the global aviation ozone perturbation (hatching indicates statistical significance at the 0.05 level).

We also compare temperature responses to aviation BC simulated by HadSM3 using the same model configuration as given in Shine et al. (2012).

For comparison with climate model results, we use the regional climate sensitivities to estimate a regional equilibrium temperature response ($\Delta T_{i,r,m}$) rather than the temperature response over time, i.e., assuming a constant forcing, following Eq. 6 of Shindell (2012):

$$\Delta T_{i,r,m} = \sum_l RF_{l,r} \cdot RCS_{i,l,m} \cdot ECS \quad (8)$$

Earth Syst. Dynam. Discuss., doi:10.5194/esd-2017-11, 2017
Manuscript under review for journal Earth Syst. Dynam.
Published: 7 February 2017

286 adopting the equilibrium climate sensitivity (ECS) from Boucher and Reddy (2008) described
287 above.

288

289 **3 RESULTS AND DISCUSSION**

290 **3.1 GLOBAL EMISSION METRICS**

291 Tables 1 and 2 summarize the 20 and 100 year GWPs and GTPs of global and regional aviation
292 emissions, respectively, given relative to CO_2 using the CO_2 impulse response function (IRF_{CO2})
293 from Joos et al. (2013). The global GWPs and GTPs are not the main focus of our study, but are
294 included and briefly described for comparison with previous estimates.

295 Our GWPs for the net effect of global aviation NOx are somewhat higher than the range estimated
296 by Skowron et al. (2013) using several different aviation emission inventories in a single model
297 and Myhre et al. (2010) based on multi-model results (Table 1). They also fall in the upper end of
298 the range reported by Fuglestvedt et al. (2010). The NOx GTPs fall at or in the positive end of
299 reported ranges. A number of factors can contribute to difference in the metric values, including
300 differences in input radiative forcing, treatment and inclusion of methane-induced changes in
301 ozone and stratospheric water vapor, and differences in the parameters of the IRF_{CO2}. The
302 estimated contrail-cirrus GWPs and GTPs are about 30 percent higher than given in Fuglestvedt
303 et al. (2010). This is unsurprising since we in the present analysis consider the RF of contrail-cirrus,
304 i.e., young line shaped contrails and those cirrus originating from them, and their associated optical
305 depth, and not only line shaped contrails as in earlier studies. The RF of contrail-cirrus was shown
306 to be 9 times higher than the RF of line shaped contrails when assuming constant optical depth
307 (Burkhardt & Kaercher, 2011). Further differences arise from the use of different IRF_{CO2}. Our
308 GWPs and GTPs for the direct effect of BC and sulfate aerosols are higher than those derived by
309 Fuglestvedt et al. (2010) by a four (a factor two for BC GTPs). However, the values from
310 Fuglestvedt et al. (2010) are not specific for aviation emissions, but based on input multi-model
311 mean RF from all anthropogenic emissions (Schulz et al., 2006). We are not aware of any previous
312 estimates of aviation aerosol GWP and GTP.

313 Quantifying the GTPs and GWPs of regional aviation emissions allows us to capture how equal
314 emissions in different locations can have different impacts on the atmospheric concentrations and

Earth Syst. Dynam. Discuss., doi:10.5194/esd-2017-11, 2017
Manuscript under review for journal Earth Syst. Dynam.
Published: 7 February 2017

315 RF, and in turn on global climate. Our calculations reveal considerable differences between regions
316 for all species, and both metrics and time horizons, with a factor 2-4 (and higher for nitrate)
317 difference between the highest and lowest metric value (Table 2). For the aerosols we generally
318 find the largest magnitude GWPs and GTPs for South Asia (SAS) emissions, followed by South
319 America and Africa (SAF) or South Pacific Ocean (SPO). The high values for the SAS region
320 reflects a relatively long lifetime of the aerosols here compared to other emission regions. This, in
321 turn, is likely caused by a combination of the underlying distribution of emissions, which is
322 dominated by high altitude emissions (i.e., few flights landing or departing within the region), and
323 the dry conditions (i.e., less wet scavenging of the aerosols) in the region. For NOx, the values
324 are highest for SPO, while for contrail-cirrus we find high values for aviation over NAM and
325 Europe (EUR), where conditions for contrail formation is prevalent (e.g., Burkhardt et al. (2008);
326 Irvine and Shine (2015)) and for SAF (see more detailed discussion in Sect. 3.2). From a policy
327 perspective, knowledge of such regional differences is important if metrics are used to quantify
328 the climate impact of emissions or emission changes in cases where there is a simultaneous change
329 in the geographical emission distribution, or if used to evaluate the effect of implementing
330 measures to reduce emissions in different regions.

331 While several studies have estimated GWPs and GTPs for global aviation NOx emissions, as
332 discussed above, few have produced estimates for regional aviation emissions. Köhler et al. (2013)
333 quantified the climate impact of aviation emissions in North America, Europe, India and China.
334 The reported GWPs and GTP(100) for emissions in India agree within 10-15 percent with
335 estimates for SAS in the present analysis. Our GTP(20) values are about 50 percent lower in
336 absolute magnitude for all emission regions, while GWP(100) and GTP(100) for NAM and EUR
337 are 50-100 percent higher than Köhler et al. (2013) estimates. Again it should be noted that these
338 difference can be caused by a number of factors. Moreover, because the two studies use differently
339 defined emission source regions, only a rough comparison is possible.

340

341 **3.2 Regional emission metrics**

342 While GWPs and GTPs illustrate how equal emissions in various regions can have different
343 impacts on global climate, they can naturally not inform us of the actual regional distribution of

Earth Syst. Dynam. Discuss., doi:10.5194/esd-2017-11, 2017
Manuscript under review for journal Earth Syst. Dynam.
Published: 7 February 2017

344 impacts. The ARTP allows us to estimate temperature impacts with at least some spatial
345 information.

346 Figure 2 shows the ARTP with a time horizon of 20 years (ARTP(20)) for BC, OC, SO_2 and
347 contrail-cirrus for each emission source region, and the ARTP(20) and ARTP(100) of aviation
348 NOx. We do not show ARTP(100) for aerosols and contrail-cirrus here. The absolute values decay
349 strongly over time, but the latitudinal patterns will be identical on both time horizons. Results for
350 global aviation emissions are given in the SI, as are contrail-cirrus metrics on a per km-basis.
351

352 For OC and SO_2 (Fig. 2B and C), we calculate the highest magnitude ARTP(20) (i.e., temperature
353 impact per unit emission) for aviation in SAS in all latitude bands except 90-28°S, where values
354 for SAF and SPO are slightly higher. Excluding the SAS region, aviation in EUR and NAM give
355 the highest temperature impact per unit emission in the 28-60°N and 60-90°N regions, which is
356 also where the corresponding RF is strongest (Table SI 2). This is unsurprising given that these
357 species are short-lived and the forcing they exert are largely localized to the emission region.
358 However, using the ARTP reveals important differences between the latitudinal distribution of RF
359 and subsequent temperature response. In given latitude bands, the temperature impact can be
360 considerably stronger than the RF in that band suggests, and can extend to the opposite hemisphere
361 to where the emissions occurred. Applying the $RCS_{i,l,m}$ given in the coarse latitude bands smooths
362 out the impacts such that there is less latitudinal variation in the temperature responses than in the
363 RFs. This illustrates the dependence of temperature response on both forcing exerted locally and
364 on remote impacts through large-scale circulation impacts and feedbacks in the climate system.
365

366 The latter effects are also very important in the case of BC (Fig. 2A). Again, the ARTP(20) is
367 highest for aviation in SAS, while the difference between remaining regions is smaller than for
368 OC and SO_2 in most latitudes bands. In the 60-90°N region, aviation in the Southern Hemispheric
369 regions cause the highest temperature per unit emissions, despite being far removed from the
370 Arctic. In the GISS results, the Arctic temperature response to local (i.e., within Arctic) forcing is
371 in fact negative (Shindell & Faluvegi, 2009). This local cooling effect applies to BC changes in
372 the mid to upper Arctic troposphere, which is where aviation is most important. Aviation BC
373 emissions in EUR and NAM are more easily transported into the Arctic region and hence induce

Earth Syst. Dynam. Discuss., doi:10.5194/esd-2017-11, 2017
Manuscript under review for journal Earth Syst. Dynam.
Published: 7 February 2017

374 a stronger local forcing and in turn a larger surface cooling. The net effect of aviation in these
375 regions on the Arctic is still a warming, but this warming is partly offset by the cooling contribution
376 from within Arctic RF. In contrast, aviation BC emissions in SAS, EAS, SAF and SPO have less
377 potential for long-range transport to the Arctic, but the remote BC forcing warms the Arctic
378 through transport of energy. In terms of mitigation, these results underline that if the goal is to
379 limit temperature increase e.g., in the Arctic, it is necessary to go beyond radiative forcing as an
380 indicator and to also consider the impact of emission in more remote regions. This feature has been
381 illustrated also for other sectors and regions (Collins et al., 2013; Lund et al., 2014).
382
383 For contrail-cirrus (Fig 2D), the ARTP(20) for aviation in EUR and NAM is substantially larger
384 in the 28-60°N and 60-90°N latitude bands than for other sources regions considered in this study,
385 while the difference between source regions is less pronounced in the Southern Hemisphere
386 latitude bands. There are two main competing processes at play. Contrail formation is generally
387 more prevalent in the extratropics due to lower temperatures at flight levels than in the tropics and
388 may persist longer due to larger probability of ice supersaturation. An upward shift in the flight
389 level increases the probability of contrails formation and ice supersaturation (Burkhardt et al.,
390 2008). It should be noted that local peaks of ice supersaturation are also found in the tropics (Irvine
391 & Shine, 2015), in fact the probability of ice supersaturation is highest in the upper tropical
392 troposphere (Lamquin et al., 2012). Furthermore, once contrails have formed contrail-cirrus, the
393 optical depth is higher in the tropics due to the larger amount of water vapor available for
394 deposition. This higher optical depth in the tropics and the consequently higher RF has also been
395 found in contrail-cirrus simulations (Burkhardt & Kaercher, 2011). However, none of our source
396 regions cover only the tropics. In the SAS region, the air is mostly too warm for contrail formation.
397 However, if contrails were present here, their radiative forcing efficiency would be high. Due to
398 the competing short- and long-wave effects, there can be important diurnal and seasonal variability
399 in the net impact of contrail-cirrus (e.g., Stuber et al. (2006); Bock and Burkhardt (2016a)). The
400 diurnal effects depends on assumptions about the contrail-cirrus lifetime and were shown to be
401 small (Newinger & Burkhardt, 2012) when using the contrail-cirrus parameterization of Burkhardt
402 and Kaercher (2011). This effect is not captured in our analysis using annual mean RF as input.
403

Earth Syst. Dynam. Discuss., doi:10.5194/esd-2017-11, 2017
Manuscript under review for journal Earth Syst. Dynam.
Published: 7 February 2017

Earth System Dynamics Discussions
Open Access
EGU

It should be emphasized that the contrail-cirrus metrics are suitable for the average of the present-day aircraft fleet. Their application would not be appropriate if there are significant changes in routes and flight altitudes. Future changes in climate may also affect the potential for contrail-cirrus formation in a given region (Irvine & Shine, 2015). As discussed in Sect. 2, several factors contribute to uncertainty in the emission metrics, and should be kept in mind in further applications.

The ARTP of aviation NOx (Fig. 2E, F) is separated into contributions from ozone, methane and methane-induced ozone, as well as the direct effect of nitrate aerosols. The stars indicate the net NOx effect. The ARTP(20) is negative in all but two cases, i.e., the net effect of one year of aviation NOx emissions is a cooling on this time scale, dominated by the NOx-induced methane loss. However, it is important to note that the sign and magnitude of the net NOx effect is very sensitive to the choice of time horizon due to the very different time scales on which the ozone and methane contributions act. In particular, during the first decade after emission, the strong but short-lived warming from ozone dominates, resulting in a net positive effect (see also Fig. 6B of Fuglestvedt et al. (2010)). Moreover, the NOx ARTP is also influenced by the spatial patterns of ozone and methane. Due to the shorter lifetime, the aviation-induced ozone perturbation is more heterogeneous than the methane concentration change, and more confined to the emission source region. The choice of time horizon may therefore affect both the net NOx effect and the relative importance of source regions. Both the impact of changes in ozone and methane from a pulse emission on NOx decays strongly over time, as reflected by the much smaller ARTP(100). While the methane cooling remains important on longer time scales, the absolute magnitude diminishes strongly towards a time horizon of 100 years. For all source regions, the competing effects of ozone warming and methane cooling over time results in a small, but net positive global mean effect of aviation NOx on a 100 year time horizon. In the 90-28°S latitude band the ARTP(100) is positive for emissions occurring in the Southern Hemisphere, but negative for emissions in the Northern Hemisphere, as the latter causes a much smaller ozone concentration change in this latitude band and the methane cooling becomes relatively more important over time. A similar response is seen in the 60-90°N latitude band.

3.3 Regional climate impacts of the present-day aviation sector

Earth Syst. Dynam. Discuss., doi:10.5194/esd-2017-11, 2017
Manuscript under review for journal Earth Syst. Dynam.
Published: 7 February 2017

To place our climate metrics in context and illustrate further application, we apply the ARTP and estimate the regional temperature responses over time to present-day aviation in the six emission source regions. Figure 3 shows the contribution to temperature response in each latitude band by species and emission region 20 and 100 years after a *one-year pulse* of present-day aviation emissions. The current aviation climate mitigation policy is largely focused on CO_2. The contributions from aviation CO_2 emissions is therefore added to place the impact of short-lived and long-lived species in context.

The majority of flights today take place over the northern mid-latitudes. As a result, the net warming is largest in all latitude bands for emissions over NAM and EUR. On a 20 year time horizon, the largest warming contribution comes from contrail-cirrus formation and, despite the highly localized RF, the temperature impact is not only limited to the latitude band closest to where the emissions occur. As noted in Sect. 2.2, studies indicate that the efficacy of contrail-cirrus may be lower than one. This is not accounted for in the current analysis, but adopting a uniform efficacy of e.g., 0.6 (Ponater et al., 2005) would result in a 40 percent lower contrail-cirrus impact across all latitude bands. The net warming is slightly offset by a small cooling due to NOx-induced methane loss, especially in the 90-28°S and 60-90°N regions. As pointed out above, the sign and magnitude of the net NOx effect depends strongly on the chosen time horizon. For instance, on a 10 year time horizon (not shown here), the net NOx response is a warming in the 28°S-28°N and 28-60°N regions for emissions in NAM, EUR and EAS. Aviation emissions of BC are small and therefore contribute little to the net impact, despite the strong efficiency (i.e., temperature change per kg emitted).

Even on short time horizons (e.g., 20 years), the warming contribution from CO_2 is important. On longer time horizons (e.g., 100 years) the impact from contrail-cirrus and NOx decays, and the CO_2 contribution becomes dominant in all latitude bands. This has previously been illustrated for the global mean temperature impact of the sector (Berntsen & Fuglestvedt, 2008). Because the perturbation in CO_2 is longer-lived and well-mixed, the warming in the Southern Hemisphere becomes relatively more important compared to the other latitude bands on longer time scales. Nevertheless, for emissions in NAM and EUR, for the northern hemisphere response regions and the global mean, the contributions from contrail-cirrus remains substantial and approximately 20 percent of the CO_2 response, even on these long time scales. Figure 3 also shows that the relative

Earth Syst. Dynam. Discuss., doi:10.5194/esd-2017-11, 2017
Manuscript under review for journal Earth Syst. Dynam.
Published: 7 February 2017

importance of the source regions across latitude bands following a pulse emission changes very little over time. However, these calculations do not account for potential future changes in the geographical distribution of emissions.

Our study focuses on the pulse based emission metrics and does not consider the future temperature impact of aviation following *emission scenarios*, which would change the timescale of the response and the relative importance of short- and long-lived species over time. As described in Sect. 2.2, our pulse based emission metrics can be used in further studies to investigate the regional temperature impacts following more realistic emission scenarios. For instance, as the simplest form of scenario, one could assume that emissions are kept constant at the present-day level. In this case, the contributions from short-lived species such as contrail-cirrus, ozone and sulfate would quickly become sustained at a constant level rather than decay towards zero and the warming from CO_2 would gradually accumulate (e.g., Berntsen and Fuglestvedt (2008)). The impact of contrail-cirrus may even increase if emissions are kept constant while fuel efficiency is improved. The temporal behavior of total net temperature response, as well as the net NOx effect, would differ notably from the pulse emission case.

3.4 EVALUATION

Several studies have used the ARTP concept to estimate temperature responses to emissions from specific sectors or regions (Collins et al., 2013; Lund et al., 2014; Stohl et al., 2015). Stohl et al. (2015) also compared the estimated temperature responses to short-lived climate pollutants to those simulated by several climate models. However, these studies focus only on surface sources. Moreover, the regional climate sensitivities that form the basis for the ARTP calculations are derived from simulations with only one climate model. They are also representative of the response to a vertical forcing profile resulting from total anthropogenic emissions, i.e., one that in many regions differ considerably from those induced by the mainly high-altitude aviation emissions. Several recent studies have found a strong vertical sensitivity in the BC forcing-response relationship, with decreasing efficacy with altitude (Ban-Weiss et al., 2011; Flanner, 2013; Samset & Myhre, 2015). Climate model studies also indicate that the forcing-response relationship for ozone will be dependent on both the vertical and horizontal distribution of the ozone change (Berntsen et al., 1997; Hansen et al., 1997; Joshi et al., 2003). In the light of the potential

Earth Syst. Dynam. Discuss., doi:10.5194/esd-2017-11, 2017
Manuscript under review for journal Earth Syst. Dynam.
Published: 7 February 2017

494 uncertainties arising from such vertical dependency, we perform a first evaluation of the ARTP
495 concept in the context of aviation ozone and BC. Further evaluation, especially of contrail-cirrus,
496 would be valuable. However, the resources for the required climate model simulations were not
497 available for this study.
498
499 Figure 4A shows the normalized regional temperature response to aviation ozone, as simulated by
500 the CESM1.2, HadSM3 and ECHAM (see Sect. 2.3) and estimated using the regional climate
501 sensitivities that form the basis for the ARTP concept. There are several factors potentially
502 contributing to differences in the absolute magnitude of temperature responses in the simulations,
503 including differences in the ozone concentration perturbation resulting from differences in
504 emissions or ozone change per unit emission, radiative efficiency and ECS. HadSM3 and ECHAM
505 used the multi-model average ozone concentration change resulting from year 2000 aviation NOx
506 emission (0.67 TgN) (Hoor et al., 2009), while this study (using CESM2.1) uses the ozone change
507 simulated by one model (OsloCTM3) and year 2006 aviation emissions (0.81 TgN). Based on
508 visual inspection, these two aviation-induced ozone concentration perturbations are quite similar,
509 with slightly larger perturbation at high northern latitudes in the present study. Nonetheless, here
510 we focus on the spatial pattern across latitude bands rather than absolute magnitudes and therefore
511 normalize the temperature response in each band by the respective global mean response.

512 The climate models and RTP agree reasonably well in the 28°S-28°N and 28-60°N latitude bands.
513 However, in both the 90-28°S and 60-90°N regions, the temperature response simulated directly
514 by the climate models is considerably higher than that estimated using the ARTP. The low ARTP-
515 derived temperature response in the 60-90°N region reflects the low sensitivity in the GISS model
516 in this latitude band to ozone forcing exerted both locally, as well as in the 28-60°N region where
517 the aviation-induced forcing is highest (Fig. 1 of Shindell and Faluvegi (2009)). A low, and even
518 negative, sensitivity to Northern Hemisphere forcing also characterizes the 90-28°S band.

519 The reason for the low sensitivity in the GISS simulations, or whether this is a feature specific to
520 this model, is not clear. It is possible that the differences between modeled and estimated
521 temperature response to aviation ozone forcing can be at least partly explained by vertical
522 variations in the response to ozone perturbations. Early work by Hansen et al. (1997) suggested a
523 surface cooling in response to a global near surface ozone perturbation and a maximum efficacy

Earth Syst. Dynam. Discuss., doi:10.5194/esd-2017-11, 2017
Manuscript under review for journal Earth Syst. Dynam.
Published: 7 February 2017

around 700-800 hPa, followed by a decreasing efficacy for ozone perturbations in the upper troposphere. The latter was supported by Joshi et al. (2003). However, the increased sensitivity to lower stratosphere perturbations found by Joshi et al. (2003) was not seen in the Hansen et al. (1997) results. Such uncertainties in the efficacy around the UTLS region are important in the case of aviation.

Figure 4B compares aviation BC temperature response to that obtained from the HadSM3. The regional distribution across latitude bands is similar for the estimated and simulated temperature response. However, here we only have temperature response simulated by one climate model. Given the substantial uncertainty and inter-model differences in model estimates of BC climate impacts (Baker et al., 2015; Samset et al., 2014; Stohl et al., 2015), additional model simulations are needed for further comparison and evaluation.

The notable decrease in BC efficacy with altitude globally, and particularly at high latitudes (Ban-Weiss et al., 2011; Flanner, 2013; Samset & Myhre, 2015), raises the question whether using the ARTP to estimate temperature responses to the high-altitude aviation BC forcing could result in an overestimation of the absolute magnitude. Flanner (2013) provided vertically resolved climate sensitivities for the Arctic temperature response to local Arctic BC forcing. Using these, Lund et al. (2014) found important differences in the temperature response to BC from on-road transportation in the 60-90°N latitude band compared to using the single regional climate sensitivity derived from Shindell and Faluvegi (2009) (and used in the present analysis). At the altitudes in the 60-90°N region where the aviation-induced RF peaks, the regional climate sensitivity from Flanner (2013) and Shindell and Faluvegi (2009), and hence the estimated temperature response, agree quite well. This agreement may not hold for all regions, but similar vertically resolved climate sensitivities for other latitude bands or species do not currently exist.

Based on our analysis, some care is needed when using the ARTP in the context of aviation emissions. Specifically, our findings suggest that the temperature response in the 90-28°S and 60-90°N regions to aviation ozone could be underestimated by the regional climate sensitivities currently used in the ARTP calculations. Furthermore, a possible overestimation of temperature response to aviation BC can not be ruled out. Further work to quantify the importance of vertical variations in forcing-response relationships and develop regional climate sensitivities based on vertically-resolved forcing perturbations would be valuable for future use of the ARTP.

Earth Syst. Dynam. Discuss., doi:10.5194/esd-2017-11, 2017
Manuscript under review for journal Earth Syst. Dynam.
Published: 7 February 2017

554

555 **4 CONCLUSIONS**

556 We have examined the impacts of aviation emissions on global and regional temperature,
557 characterizing them using emission metrics. We address the impacts of NO_x on ozone and methane,
558 aerosols and contrail-cirrus formation, and consider six emission regions spanning both
559 hemispheres. In addition to updated emission metrics for global aviation, we present GWPs and
560 GTPs on 20 and 100 year time horizons for a larger set of species and regions than previous studies.
561 We also calculate the Absolute Regional Temperature change Potential (ARTP) for aviation,
562 allowing us to not only capture how equal emissions in different regions impact global climate,
563 but also quantify the temperature impacts on a sub-global scale.

564 The metric values depend significantly on emission regions. In the case of aviation aerosols, we
565 calculate the highest GWPs and GTPs for emissions in South Asia, followed by South America
566 and Africa, and the South Pacific Ocean. The strong efficiency of emissions over our South Asian
567 region reflects a relatively long lifetime of the aerosols here compared to other region. Our results
568 do not include aerosol-cloud interactions, an important limitation as recent studies suggest aviation
569 can potentially have strong impact through modification of both cirrus and low-level clouds,
570 although this contribution remains particularly uncertain. The net temperature impact over time
571 following a pulse emission of aviation NOx is determined by the relative importance of the cooling
572 and warming methane and ozone contributions, and is very sensitive to the choice of time horizon.
573 The net NOx ARTP is negative after 20 years and switches to a small net warming on a 100 year
574 time horizon on global mean and in the latitude band closest to the where the emission occur.
575 Metrics for contrail-cirrus are calculated on a per unit emission of aviation CO_2 basis. The GWPs
576 and GTPs are highest for North America and Europe, where contrail-cirrus formation is prevalent.
577 However, once formed, contrail-cirrus in the tropics have much higher optical depth due to the
578 larger amount of water vapor. The metric values do not account for a lower efficacy of contrail-
579 cirrus suggested by previous studies. Moreover, the contrail-cirrus metrics would not be
580 appropriate if there are significant changes in routes and flight altitudes, or if changes in climate
581 or propulsion efficiency affect the potential for contrail-cirrus formation.
582

Earth Syst. Dynam. Discuss., doi:10.5194/esd-2017-11, 2017
Manuscript under review for journal Earth Syst. Dynam.
Published: 7 February 2017

583 The ARTPs illustrate how the latitudinal temperature pattern can differ significantly from the
584 global mean, as well as from the latitudinal pattern of RF. Due to the short lifetime of many of the
585 aviation forcing mechanisms, the RF is typically largely confined to the latitude band closest to
586 where the emissions occur. However, in a given latitude band, the temperature response can be
587 considerably stronger than suggested by the corresponding forcing, emphasizing the importance
588 of both forcing exerted locally and remote impacts through large-scale circulation impacts and
589 feedbacks in the climate system.
590
591 While the strongest efficiency (temperature change per kg emitted) of aviation aerosols and NOx
592 is found for emissions in the South Asian region in our study, the majority of flights today take
593 place over the northern mid-latitudes. The net warming impact 20 and 100 years following a one-
594 year pulse emission from the present-day aviation sector is therefore largest in all latitude bands
595 for emissions in North America and Europe. For all regions, the largest warming contribution is
596 from contrail-cirrus on a 20 year time horizon. While CO_2 becomes dominant on the 100 year time
597 horizon, contributions from contrail-cirrus remains important on the 20 percent of CO_2 level in
598 several regions even on these long time scales. Our metric framework can also be applied to
599 estimate future regional temperature impact of more realistic emissions scenarios for the sector,
600 which would influence the temporal characteristic of the response and the relative contributions of
601 short and long-lived species over time.

602 While the ARTP concept is an important and useful tool for providing first order estimates of
603 regional temperature of various emissions, our analysis indicate that some care is needed when it
604 is used in the context of aviation emissions, or more generally, in situations that differ significantly
605 from those used to derive the regional climate sensitivities for the ARTP calculations in the first
606 place. In particular, further work to quantify and account for the relationship between vertically-
607 resolved radiative forcing perturbations and surface temperature response is needed to allow for a
608 more general applicability of the concept.

609

610

611

Earth Syst. Dynam. Discuss., doi:10.5194/esd-2017-11, 2017
Manuscript under review for journal Earth Syst. Dynam.
Published: 7 February 2017

Earth System Dynamics Discussions Open Access EGU

Acknowledgements

This is work funded by the US Federal Aviation Administration (FAA)/Volpe Center under the contract no. DTRT57-12-P-80123. We thank Dr. Øivind Hodnebrog (CICERO) for contributions.

References

Aamaas B., Peters G. P. & Fuglestvedt J. S. (2013). Simple emission metrics for climate impacts. *Earth System Dynamics.* 4(1), 145-170, DOI: 10.5194/esd-4-145-2013.

Aamaas B., Berntsen T. K., Fuglestvedt J. S., Shine K. P. & Bellouin N. (2016). Regional emission metrics for short-lived climate forcers from multiple models. *Atmos. Chem. Phys.* 16(11), 7451-7468, DOI: 10.5194/acp-16-7451-2016.

Baker L. H., Collins W. J., Olivié D. J. L., Cherian R., Hodnebrog Ø., Myhre G. & Quaas J. (2015). Climate responses to anthropogenic emissions of short-lived climate pollutants. *Atmos. Chem. Phys.* 15(14), 8201-8216, DOI: 10.5194/acp-15-8201-2015.

Ban-Weiss G., Cao L., Bala G. & Caldeira K. (2011). Dependence of climate forcing and response on the altitude of black carbon aerosols. *Climate Dynamics*, 1-15, DOI: 10.1007/s00382-011-1052-y.

Berntsen T. & Fuglestvedt J. (2008). Global temperature responses to current emissions from the transport sectors. *Proceedings of the National Academy of Sciences of the United States of America.* 105(49), 19154-19159, DOI: 10.1073/pnas.0804844105.

Berntsen T. K., Isaksen I. S. A., Myhre G., Fuglestvedt J. S., Stordal F., Larsen T. A., Freckleton R. S. & Shine K. P. (1997). Effects of anthropogenic emissions on tropospheric ozone and its radiative forcing. *Journal of Geophysical Research: Atmospheres.* 102(D23), 28101-28126, DOI: 10.1029/97JD02226.

Bindoff N. L., Stott P. A., AchutaRao K. M., Allen M. R., Gillett N., Gutzler D., Hansingo K., Hegerl G., Hu Y., Jain S., Mokhov I. I., Overland J., Perlwitz J., Sebbari R. & Zhang X. (2013). Detection and Attribution of Climate Change: from Global and Regional. In: Climate Change 2013: The Physical Science Basis. Contribution of Working Group I to the Fifth Assessment Report of the Intergovernmental Panel on Climate Change [Stocker, T.F., D. Qin, G.-K. Plattner, M. Tignor, S.K. Allen, J. Boschung, A. Nauels, Y. Xia, V. Bex and P.M. Midgley (eds.)]. Cambridge University Press, Cambridge, United Kingdom and New York, NY, USA.

Bock L. & Burkhardt U. (2016a). Reassessing properties and radiative forcing of contrail cirrus using a climate model. *Journal of Geophysical Research: Atmospheres.* 121(16), 9717-9736, DOI: 10.1002/2016JD025112.

Bock L. & Burkhardt U. (2016b). The temporal evolution of a long-lived contrail cirrus cluster: Simulations with a global climate model. *Journal of Geophysical Research: Atmospheres.* 121(7), 3548-3565, DOI: 10.1002/2015JD024475.

Boer G. J. & Yu B. (2003). Climate sensitivity and response. *Climate Dynamics.* 20(4), 415-429, DOI: 10.1007/s00382-002-0283-3.

Boucher O. & Reddy M. S. (2008). Climate trade-off between black carbon and carbon dioxide emissions. *Energy Policy.* 36(1), 193-200, DOI: 10.1016/j.enpol.2007.08.039.

Brasseur G. P., Gupta M., Anderson B. E., Balasubramanian S., Barrett S., Duda D., Fleming G., Forster P. M., Fuglestvedt J., Gettelman A., Halthore R. N., Jacob S. D., Jacobson M. Z., Khodayari A., Liou K.-N., Lund M. T., Miake-Lye R. C., Minnis P., Olsen S., Penner J. E., Prinn R., Schumann U., Selkirk H. B.,

654 Sokolov A., Unger N., Wolfe P., Wong H.-W., Wuebbles D. W., Yi B., Yang P. & Zhou C. (2016). Impact of
655 Aviation on Climate: FAA's Aviation Climate Change Research Initiative (ACCRI) Phase II. *Bulletin of the*
656 *American Meteorological Society.* 97(4), 561-583, DOI: 10.1175/bams-d-13-00089.1.
657 Burkhardt U., Kärcher B., Ponater M., Gierens K. & Gettelman A. (2008). Contrail cirrus
658 supporting areas in model and observations. *Geophysical Research Letters.* 35(16), n/a-n/a, DOI:
659 10.1029/2008GL034056.
660 Burkhardt U. & Kaercher B. (2011). Global radiative forcing from contrail cirrus. *Nature Climate*
661 *Change.* 1(1), 54-58, DOI: 10.1038/nclimate1068.
662 Collins W. J., Fry M. M., Yu H., Fuglestvedt J. S., Shindell D. T. & West J. J. (2013). Global and
663 regional temperature-change potentials for near-term climate forcers. *Atmos. Chem. Phys.* 13(5), 2471-
664 2485, DOI: 10.5194/acp-13-2471-2013.
665 Fahey D. W., Keim E. R., Boering K. A., Brock C. A., Wilson J. C., Jonsson H. H., Anthony S.,
666 Hanisco T. F., Wennberg P. O., Miake-Lye R. C., Salawitch R. J., Louisnard N., Woodbridge E. L., Gao R. S.,
667 Donnelly S. G., Wamsley R. C., Del Negro L. A., Solomon S., Daube B. C., Wofsy S. C., Webster C. R., May
668 R. D., Kelly K. K., Loewenstein M., Podolske J. R. & Chan K. R. (1995). Emission Measurements of the
669 Concorde Supersonic Aircraft in the Lower Stratosphere. *Science.* 270(5233), 70-74, DOI:
670 10.1126/science.270.5233.70.
671 Flanner M. G. (2013). Arctic climate sensitivity to local black carbon. *Journal of Geophysical*
672 *Research-Atmospheres.* 118(4), 1840-1851, DOI: 10.1002/jgrd.50176.
673 Fry M. M., Naik V., West J. J., Schwarzkopf M. D., Fiore A. M., Collins W. J., Dentener F. J.,
674 Shindell D. T., Atherton C., Bergmann D., Duncan B. N., Hess P., MacKenzie I. A., Marmer E., Schultz M.
675 G., Szopa S., Wild O. & Zeng G. (2012). The influence of ozone precursor emissions from four world
676 regions on tropospheric composition and radiative climate forcing. *Journal of Geophysical Research-*
677 *Atmospheres.* 117, D07306, DOI: 10.1029/2011jd017134.
678 Fuglestvedt J. S., Berntsen T. K., Godal O., Sausen R., Shine K. P. & Skodvin T. (2003). Metrics of
679 climate change: Assessing radiative forcing and emission indices. *Climatic Change.* 58(3), 267-331.
680 Fuglestvedt J. S., Shine K. P., Berntsen T., Cook J., Lee D. S., Stenke A., Skeie R. B., Velders G. J. M.
681 & Waitz I. A. (2010). Transport impacts on atmosphere and climate: Metrics. *Atmospheric Environment.*
682 44(37), 4648-4677, DOI: 10.1016/j.atmosenv.2009.04.044.
683 Gettelman A. & Chen C. (2013). The climate impact of aviation aerosols. *Geophysical Research*
684 *Letters.* 40(11), 2785-2789, DOI: 10.1002/grl.50520.
685 Gilmore C. K., Barrett S. R. H., Koo J. & Wang Q. (2013). Temporal and spatial variability in the
686 aviation NOx-related O-3 impact. *Environmental Research Letters.* 8(3), 034027, DOI: 10.1088/1748-
687 9326/8/3/034027.
688 Hansen J., Sato M. & Ruedy R. (1997). Radiative forcing and climate response. *Journal of*
689 *Geophysical Research: Atmospheres.* 102(D6), 6831-6864, DOI: 10.1029/96JD03436.
690 Holmes C. D., Prather M. J., Sovde O. A. & Myhre G. (2013). Future methane, hydroxyl, and their
691 uncertainties: key climate and emission parameters for future predictions. *Atmospheric Chemistry and*
692 *Physics.* 13(1), 285-302, DOI: 10.5194/acp-13-285-2013.
693 Hoor P., Borken-Kleefeld J., Caro D., Dessens O., Endresen O., Gauss M., Grewe V., Hauglustaine
694 D., Isaksen I. S. A., JÃ¶ckel P., Lelieveld J., Myhre G., Meijer E., Olivie D., Prather M., Schnadt Poberaj C.,
695 Shine K. P., Staehelin J., Tang Q., van Aardenne J., van Velthoven P. & Sausen R. (2009). The impact of
696 traffic emissions on atmospheric ozone and OH: results from QUANTIFY. *Atmos. Chem. Phys.* 9(9), 3113-
697 3136.
698 Hurrell J. W., Holland M. M., Gent P. R., Ghan S., Kay J. E., Kushner P. J., Lamarque J.-F., Large W.
699 G., Lawrence D., Lindsay K., Lipscomb W. H., Long M. C., Mahowald N., Marsh D. R., Neale R. B., Rasch P.,
700 Vavrus S., Vertenstein M., Bader D., Collins W. D., Hack J. J., Kiehl J. & Marshall S. (2013). The

701 Community Earth System Model: A Framework for Collaborative Research. *Bulletin of the American*
702 *Meteorological Society.* 94(9), 1339-1360, DOI: doi:10.1175/BAMS-D-12-00121.1.
703 Huszar P., Teyssèdre H., Michou M., Voldoire A., Olivié D. J. L., Saint-Martin D., Cariolle D., Senesi
704 S., Salas Y Melia D., Alias A., Karcher F., Ricaud P. & Halenka T. (2013). Modeling the present and future
705 impact of aviation on climate: an AOGCM approach with online coupled chemistry. *Atmos. Chem. Phys.*
706 13(19), 10027-10048, DOI: 10.5194/acp-13-10027-2013.
707 IPCC (2014). Climate Change 2013: The Physical Science Basis. Contribution of Working Group I
708 to the Fifth Assessment Report of the Intergovernmental Panel on Climate Change [Stocker, T.F., D. Qin,
709 G.-K. Plattner, M. Tignor, S.K. Allen, J. Boschung, A. Nauels, Y. Xia, V. Bex and P.M. Midgley (eds.)].
710 Cambridge University Press, Cambridge, United Kingdom and New York, NY, USA, 1535 pp.
711 Irvine E. A. & Shine K. P. (2015). Ice supersaturation and the potential for contrail formation in a
712 changing climate. *Earth Syst. Dynam.* 6(2), 555-568, DOI: 10.5194/esd-6-555-2015.
713 Jacobson M. Z., Wilkerson J. T., Balasubramanian S., Cooper W. W., Jr. & Mohleji N. (2012). The
714 effects of rerouting aircraft around the arctic circle on arctic and global climate. *Climatic Change.* 115(3-
715 4), 709-724, DOI: 10.1007/s10584-012-0462-0.
716 Janssens-Maenhout G., Crippa M., Guizzardi D., Dentener F., Muntean M., Pouliot G., Keating T.,
717 Zhang Q., Kurokawa J., Wankmüller R., Denier van der Gon H., Kuenen J. J. P., Klimont Z., Frost G., Darras
718 S., Koffi B. & Li M. (2015). HTAP_v2.2: a mosaic of regional and global emission grid maps for 2008 and
719 2010 to study hemispheric transport of air pollution. *Atmos. Chem. Phys.* 15(19), 11411-11432, DOI:
720 10.5194/acp-15-11411-2015.
721 Joos F., Roth R., Fuglestvedt J. S., Peters G. P., Enting I. G., von Bloh W., Brovkin V., Burke E. J.,
722 Eby M., Edwards N. R., Friedrich T., Frölicher T. L., Halloran P. R., Holden P. B., Jones C., Kleinen T.,
723 Mackenzie F. T., Matsumoto K., Meinshausen M., Plattner G. K., Reisinger A., Segschneider J., Shaffer G.,
724 Steinacher M., Strassmann K., Tanaka K., Timmermann A. & Weaver A. J. (2013). Carbon dioxide and
725 climate impulse response functions for the computation of greenhouse gas metrics: a multi-model
726 analysis. *Atmos. Chem. Phys.* 13(5), 2793-2825, DOI: 10.5194/acp-13-2793-2013.
727 Joshi M., Shine K., Ponater M., Stuber N., Sausen R. & Li L. (2003). A comparison of climate
728 response to different radiative forcings in three general circulation models: towards an improved metric
729 of climate change. *Climate Dynamics.* 20(7-8), 843-854, DOI: 10.1007/s00382-003-0305-9.
730 Kapadia Z. Z., Spracklen D. V., Arnold S. R., Borman D. J., Mann G. W., Pringle K. J., Monks S. A.,
731 Reddington C. L., Benduhn F., Rap A., Scott C. E., Butt E. W. & Yoshioka M. (2016). Impacts of aviation
732 fuel sulfur content on climate and human health. *Atmos. Chem. Phys.* 16(16), 10521-10541, DOI:
733 10.5194/acp-16-10521-2016.
734 Khodayari A., Wuebbles D. J., Olsen S. C., Fuglestvedt J. S., Berntsen T., Lund M. T., Waitz I.,
735 Wolfe P., Forster P. M., Meinshausen M., Lee D. S. & Lim L. L. (2013). Intercomparison of the capabilities
736 of simplified climate models to project the effects of aviation CO2 on climate. *Atmospheric*
737 *Environment.* 75, 321-328, DOI: 10.1016/j.atmosenv.2013.03.055.
738 Köhler M. O., Raedel G., Shine K. P., Rogers H. L. & Pyle J. A. (2013). Latitudinal variation of the
739 effect of aviation NOx emissions on atmospheric ozone and methane and related climate metrics.
740 *Atmospheric Environment.* 64, 1-9, DOI: 10.1016/j.atmosenv.2012.09.013.
741 Lamquin N., Stubenrauch C. J., Gierens K., Burkhardt U. & Smit H. (2012). A global climatology of
742 upper-tropospheric ice supersaturation occurrence inferred from the Atmospheric Infrared Sounder
743 calibrated by MOZAIC. *Atmos. Chem. Phys.* 12(1), 381-405, DOI: 10.5194/acp-12-381-2012.
744 Lee D. S., Fahey D. W., Forster P. M., Newton P. J., Wit R. C. N., Lim L. L., Owen B. & Sausen R.
745 (2009). Aviation and global climate change in the 21st century. *Atmospheric Environment.* 43(22-23),
746 3520-3537, DOI: 10.1016/j.atmosenv.2009.04.024.

Lund M. T., Berntsen T., Fuglestvedt J. S., Ponater M. & Shine K. P. (2012). How much information is lost by using global-mean climate metrics? an example using the transport sector. *Climatic Change.* 113(3-4), 949-963, DOI: 10.1007/s10584-011-0391-3.

Lund M. T., Berntsen T. K., Heyes C., Klimont Z. & Samset B. H. (2014). Global and regional climate impacts of black carbon and co-emitted species from the on-road diesel sector. *Atmospheric Environment.* 98, 50-58, DOI: http://dx.doi.org/10.1016/j.atmosenv.2014.08.033.

Marais K., Lukachko S. P., Jun M., Mahashabde A. & Waitz I. A. (2008). Assessing the impact of aviation on climate. *Meteorologische Zeitschrift.* 17(2), 157-172, DOI: 10.1127/0941-2948/2008/0274.

Myhre G., Karlsdóttir S., Isaksen I. S. A. & Stordal F. (2000). Radiative forcing due to changes in tropospheric ozone in the period 1980 to 1998. *J. Geophys. Res.* 105(D23), 28935-28942, DOI: doi:10.1029/2000JD900187.

Myhre G., Nilsen J. S., Gulstad L., Shine K. P., Rognerud B. & Isaksen I. S. A. (2007). Radiative forcing due to stratospheric water vapour from CH4 oxidation. *Geophysical Research Letters.* 34(1), n/a-n/a, DOI: 10.1029/2006GL027472.

Myhre G., Shine K. P., Rädel G., Gauss M., Isaksen I. S. A., Tang Q., Prather M. J., Williams J., van Velthoven P., Dessens O., Koffi B., Szopa S., Hoor P., Grewe V. & Borken-Kleefeld J. (2010). Radiative forcing due to changes in ozone and methane caused by the transport sector. *In prep.*

Newinger C. & Burkhardt U. (2012). Sensitivity of contrail cirrus radiative forcing to air traffic scheduling. *Journal of Geophysical Research: Atmospheres.* 117(D10), n/a-n/a, DOI: 10.1029/2011JD016736.

Olivié D. J. L., Cariolle D., Teyssèdre H., Salas D., Voldoire A., Clark H., Saint-Martin D., Michou M., Karcher F., Balkanski Y., Gauss M., Dessens O., Koffi B. & Sausen R. (2012). Modeling the climate impact of road transport, maritime shipping and aviation over the period 1860–2100 with an AOGCM. *Atmos. Chem. Phys.* 12(3), 1449-1480, DOI: 10.5194/acp-12-1449-2012.

Olsen S. C., Brasseur G. P., Wuebbles D. J., Barrett S. R. H., Dang H., Eastham S. D., Jacobson M. Z., Khodayari A., Selkirk H., Sokolov A. & Unger N. (2013). Comparison of model estimates of the effects of aviation emissions on atmospheric ozone and methane. *Geophysical Research Letters.* 40(22), 6004-6009, DOI: 10.1002/2013GL057660.

Penner J. E., Lister D. H., Griggs D. J., Dokken D. J. & McFarland M. (1999), *Aviation and the global atmosphere*, 365 pp., Cambridge Univ. Press, Cambridge.

Ponater M., Marquart S., Sausen R. & Schumann U. (2005). On contrail climate sensitivity. *Geophysical Research Letters.* 32(10), n/a-n/a, DOI: 10.1029/2005GL022580.

Ponater M., Dietmüller S., Stuber N., Shine K. P., Highwood E. J. & Rädel G. (2009), Indications of distinctive efficacies for transport related ozone perturbations, paper presented at Second International Conference on Transport, Atmosphere and Climate (TAC-2), June 22-25 2009, Aachen and Maastricht.

Rap A., Forster P. M., Haywood J. M., Jones A. & Boucher O. (2010). Estimating the climate impact of linear contrails using the UK Met Office climate model. *Geophys. Res. Lett., doi:10.1029/2010GL045161, in press.* .

Righi M., Hendricks J. & Sausen R. (2016). The global impact of the transport sectors on atmospheric aerosol in 2030 - Part 2: Aviation. *Atmos. Chem. Phys.* 16(7), 4481-4495, DOI: 10.5194/acp-16-4481-2016.

Samset B. H. & Myhre G. (2011). Vertical dependence of black carbon, sulphate and biomass burning aerosol radiative forcing. *Geophysical Research Letters.* 38, L24802, DOI: 10.1029/2011gl049697.

Samset B. H., Myhre G., Herber A., Kondo Y., Li S. M., Moteki N., Koike M., Oshima N., Schwarz J. P., Balkanski Y., Bauer S. E., Bellouin N., Berntsen T. K., Bian H., Chin M., Diehl T., Easter R. C., Ghan S. J., Iversen T., Kirkevåg A., Lamarque J. F., Lin G., Liu X., Penner J. E., Schulz M., Seland Ø., Skeie R. B., Stier P., Takemura T., Tsigaridis K. & Zhang K. (2014). Modelled black carbon radiative forcing and

795 atmospheric lifetime in AeroCom Phase II constrained by aircraft observations. *Atmos. Chem. Phys.*
796 14(22), 12465-12477, DOI: 10.5194/acp-14-12465-2014.
797 Samset B. H. & Myhre G. (2015). Climate response to externally mixed black carbon as a
798 function of altitude. *Journal of Geophysical Research: Atmospheres.* 120(7), 2913-2927, DOI:
799 10.1002/2014JD022849.
800 Sausen R., Isaksen I., Grewe V., Hauglustaine D., Lee D. S., Myhre G., Kohler M. O., Pitari G.,
801 Schumann U., Stordal F. & Zerefos C. (2005). Aviation radiative forcing in 2000: An update on IPCC
802 (1999). *Meteorologische Zeitschrift.* 14(4), 555-561, DOI: 10.1127/0941-2948/2005/0049.
803 Schulz M., Textor C., Kinne S., Balkanski Y., Bauer S., Berntsen T., Berglen T., Boucher O.,
804 Dentener F., Guibert S., Isaksen I. S. A., Iversen T., Koch D., Kirkevag A., Liu X., Montanaro V., Myhre G.,
805 Penner J. E., Pitari G., Reddy S., Seland O., Stier P. & Takemura T. (2006). Radiative forcing by aerosols as
806 derived from the AeroCom present-day and pre-industrial simulations. *Atmospheric Chemistry and*
807 *Physics.* 6, 5225-5246, DOI: 10.5194/acp-6-5225-2006.
808 Shindell D. & Faluvegi G. (2009). Climate response to regional radiative forcing during the
809 twentieth century. *Nature Geoscience.* 2(4), 294-300, DOI: 10.1038/ngeo473.
810 Shindell D. & Faluvegi G. (2010). The net climate impact of coal-fired power plant emissions.
811 *Atmospheric Chemistry and Physics.* 10(7), 3247-3260.
812 Shindell D., Schulz M., Ming Y., Takemura T., Faluvegi G. & Ramaswamy V. (2010). Spatial scales
813 of climate response to inhomogeneous radiative forcing. *J. Geophys. Res.* 115(D19), D19110, DOI:
814 10.1029/2010jd014108.
815 Shindell D. T. (2012). Evaluation of the absolute regional temperature potential. *Atmospheric*
816 *Chemistry and Physics.* 12(17), 7955-7960, DOI: 10.5194/acp-12-7955-2012.
817 Shine K. P., Berntsen T. K., Fuglestvedt J. S. & Sausen R. (2005a). Scientific issues in the design of
818 metrics for inclusion of oxides of nitrogen in global climate agreements. *Proceedings of the National*
819 *Academy of Sciences of the United States of America.* 102(44), 15768-15773, DOI:
820 10.1073/pnas.0506865102.
821 Shine K. P., Fuglestvedt J. S., Hailemariam K. & Stuber N. (2005b). Alternatives to the global
822 warming potential for comparing climate impacts of emissions of greenhouse gases. *Climatic Change.*
823 68(3), 281-302, DOI: 10.1007/s10584-005-1146-9.
824 Shine K. P., Highwood E. J., Rädel G., Stuber N. & Balkanski Y. (2012). Climate model calculations
825 of the impact of aerosols from road transport and shipping. *Atmospheric and Oceanic Optics.* 25(1), 62-
826 70, DOI: 10.1134/s1024856012010125.
827 Skeie R. B., Fuglestvedt J., Berntsen T., Lund M. T., Myhre G. & Rypdal K. (2009). Global
828 temperature change from the transport sectors: Historical development and future scenarios.
829 *Atmospheric Environment.* 43, 6260-6270.
830 Skowron A., Lee D. S. & De León R. R. (2013). The assessment of the impact of aviation NOx on
831 ozone and other radiative forcing responses – The importance of representing cruise altitudes
832 accurately. *Atmospheric Environment.* 74, 159-168, DOI:
833 http://dx.doi.org/10.1016/j.atmosenv.2013.03.034.
834 Stenke A., Grewe V. & Ponater M. (2008). Lagrangian transport of water vapor and cloud water
835 in the ECHAM4 GCM and its impact on the cold bias. *Climate Dynamics.* 31(5), 491-506, DOI:
836 10.1007/s00382-007-0347-5.
837 Stevenson D. S. & Derwent R. G. (2009). Does the location of aircraft nitrogen oxide emissions
838 affect their climate impact? *Geophysical Research Letters.* 36, L17810, DOI: 10.1029/2009gl039422.
839 Stohl A., Aamaas B., Amann M., Baker L. H., Bellouin N., Berntsen T. K., Boucher O., Cherian R.,
840 Collins W., Daskalakis N., Dusinska M., Eckhardt S., Fuglestvedt J. S., Harju M., Heyes C., Hodnebrog Ø.,
841 Hao J., Im U., Kanakidou M., Klimont Z., Kupiainen K., Law K. S., Lund M. T., Maas R., MacIntosh C. R.,
842 Myhre G., Myriokefalitakis S., Olivié D., Quaas J., Quennehen B., Raut J. C., Rumbold S. T., Samset B. H.,

843 Schulz M., Seland Ø., Shine K. P., Skeie R. B., Wang S., Yttri K. E. & Zhu T. (2015). Evaluating the climate
844 and air quality impacts of short-lived pollutants. *Atmos. Chem. Phys.* 15(18), 10529-10566, DOI:
845 10.5194/acp-15-10529-2015.
846 Stuber N., Forster P., Rädel G. & Shine K. (2006). The importance of the diurnal and annual cycle
847 of air traffic for contrail radiative forcing. *Nature.* 441(7095), 864-867.
848 Søvde O. A., Prather M. J., Isaksen I. S. A., Berntsen T. K., Stordal F., Zhu X., Holmes C. D. & Hsu J.
849 (2012). The chemical transport model Oslo CTM3. *Geosci. Model Dev.* 5(6), 1441-1469, DOI:
850 10.5194/gmd-5-1441-2012.
851 Unger N., Zhao Y. & Dang H. (2013). Mid-21st century chemical forcing of climate by the civil
852 aviation sector. *Geophysical Research Letters.* 40(3), 641-645, DOI: 10.1002/grl.50161.
853 van der Werf G. R., Randerson J. T., Giglio L., Collatz G. J., Mu M., Kasibhatla P. S., Morton D. C.,
854 DeFries R. S., Jin Y. & van Leeuwen T. T. (2010). Global fire emissions and the contribution of
855 deforestation, savanna, forest, agricultural, and peat fires (1997–2009). *Atmos. Chem. Phys.* 10(23),
856 11707-11735, DOI: 10.5194/acp-10-11707-2010.
857 Wild O., Prather M. J. & Akimoto H. (2001). Indirect long-term global radiative cooling from NOx
858 Emissions. *Geophysical Research Letters.* 28(9), 1719-1722, DOI: 10.1029/2000GL012573.
859 Wilkerson J. T., Jacobson M. Z., Malwitz A., Balasubramanian S., Wayson R., Fleming G., Naiman
860 A. D. & Lele S. K. (2010). Analysis of emission data from global commercial aviation: 2004 and 2006.
861 *Atmos. Chem. Phys.* 10(13), 6391-6408, DOI: 10.5194/acp-10-6391-2010.
862 Wilks D. S. (2006). On "Field Significance" and the False Discovery Rate. *Journal of Applied*
863 *Meteorology and Climatology.* 45(9), 1181-1189, DOI: doi:10.1175/JAM2404.1.
864 Williams K. D., Senior C. A. & Mitchell J. F. B. (2001). Transient climate change in the Hadley
865 Centre models: The role of physical processes. *Journal of Climate.* 14(12), 2659-2674.
866 Zhou C. & Penner J. E. (2014). Aircraft soot indirect effect on large-scale cirrus clouds: Is the
867 indirect forcing by aircraft soot positive or negative? *Journal of Geophysical Research: Atmospheres.*
868 119(19), 11,303-311,320, DOI: 10.1002/2014JD021914.

869

870

871

872

873

874

875

876

877

878

Earth Syst. Dynam. Discuss., doi:10.5194/esd-2017-11, 2017
Manuscript under review for journal Earth Syst. Dynam.
Published: 7 February 2017

Earth System Dynamics
Discussions
Open Access
EGU

879 **Tables**

880 *Table 1: GWP and GTP of global aviation emissions for time horizons 20 and 100 years. Values*
881 *are given on a per unit aviation emission basis (contrail-cirrus calculated per kg aviation CO_2,*
882 *NOx and nitrate per kg N). The GTPs are calculated using the impulse response function by*
883 *Boucher and Reddy (2008). For comparison, aviation NOx GWP and GTP values from three*
884 *previous studies are also included.*

	GWP		GTP	
Component	**H=20**	**H=100**	**H=20**	**H=100**
Contrail-cirrus	3.9	1.05	1.12	0.14
NOx	349	55	-197	5
BC	6330	1720	1140	147
SO_2	-559	-152	-162	-21
Nitrate	-16	-4.3	-4.6	-0.59
OC	-282	-77	-82	-11
NOx				
Fuglesvedt et al. (2010)	120 to 470	-2.1 to 71	-590 to -200	-9.5 to 7.6
Myhre et al. (2011)	92 to 338	-21 to 67	-396 to -121	-5.8 to 7.9
Skowron et al. (2013)	142 to 332	4 to 60		

885

886

887

888

889

890

891

892

893

894

Earth Syst. Dynam. Discuss., doi:10.5194/esd-2017-11, 2017
Manuscript under review for journal Earth Syst. Dynam.
Published: 7 February 2017

Earth System Dynamics
Discussions
Open Access
EGU

895 *Table 2: GWP and GTP of regional aviation emissions for time horizons 20 and 100 years. Values*
896 *are given on a per unit aviation emission basis (contrail-cirrus per kg CO_2, NOx and nitrate per*
897 *kg N). The GTPs are calculated using the impulse response function by Boucher and Reddy (2008).*

		GWP		GTP	
Component	**Source region**	**H=20**	**H=100**	**H=20**	**H=100**
Contrail-cirrus	SAF	4.5	1.2	1.3	0.17
	NAM	4.2	1.1	1.2	0.16
	EAS	2.1	0.56	0.60	0.08
	EUR	3.1	0.84	0.89	0.12
	SPO	2.9	0.79	0.84	0.11
	SAS	3.2	0.88	0.93	0.12
NOx	SAF	351	25	-430	-0.6
	NAM	230	30	-175	2.3
	EAS	448	86	-136	10
	EUR	185	27	-119	2.4
	SPO	809	160	-204	19
	SAS	734	148	-165	17
BC	SAF	8810	2390	1570	203
	NAM	5780	1570	1030	133
	EAS	6770	1840	1210	156
	EUR	4860	1320	871	112
	SPO	8010	2180	1430	185
	SAS	13300	3630	2390	309
SO2	SAF	-833	-227	-242	-31
	NAM	-550	-150	-159	-21
	EAS	-602	-164	-175	-23
	EUR	-378	-103	-110	-14
	SPO	-746	-203	-216	-28
	SAS	-1120	-304	-324	-42
Nitrate	SAF	-8.6	-2.3	-2.5	-0.32
	NAM	-13	-3.4	-3.7	-0.47
	EAS	-7.4	-2.0	-2.1	-0.28
	EUR	-20	-5.5	-5.9	-0.76
	SPO	-3.3	-0.89	-0.95	-0.12
	SAS	-39	-11	-11	-1.5
OC	SAF	-481	-131	-140	-18
	NAM	-289	-79	-84	-11
	EAS	-283	-77	-82	-11
	EUR	-197	-54	-57	-7.4
	SPO	-419	-114	-122	-16
	SAS	-611	-166	-177	-23

898

Earth Syst. Dynam. Discuss., doi:10.5194/esd-2017-11, 2017
Manuscript under review for journal Earth Syst. Dynam.
Published: 7 February 2017

Earth System Dynamics
Discussions
Open Access
EGU

899

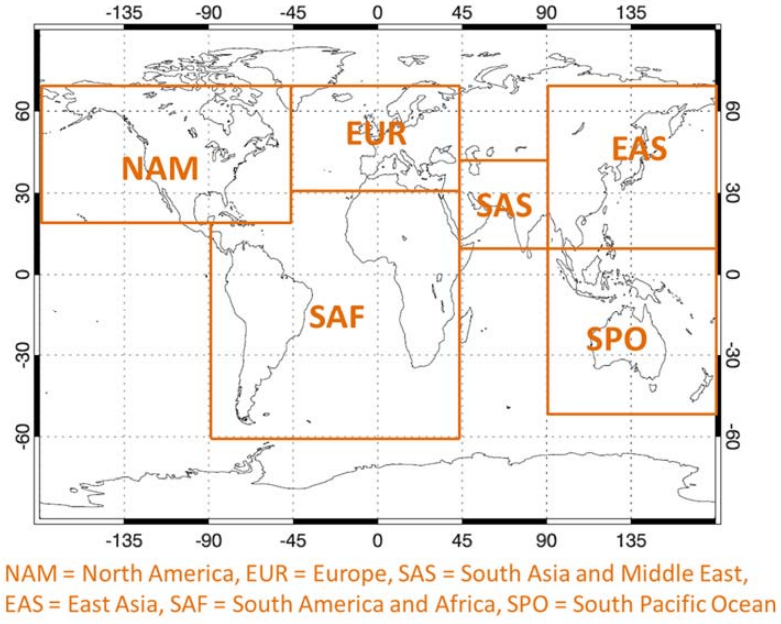

900

901 *Figure 1: Definition of emission source regions in this study.*

902

903

904

905

906

907

908

909

Earth Syst. Dynam. Discuss., doi:10.5194/esd-2017-11, 2017
Manuscript under review for journal Earth Syst. Dynam.
Published: 7 February 2017

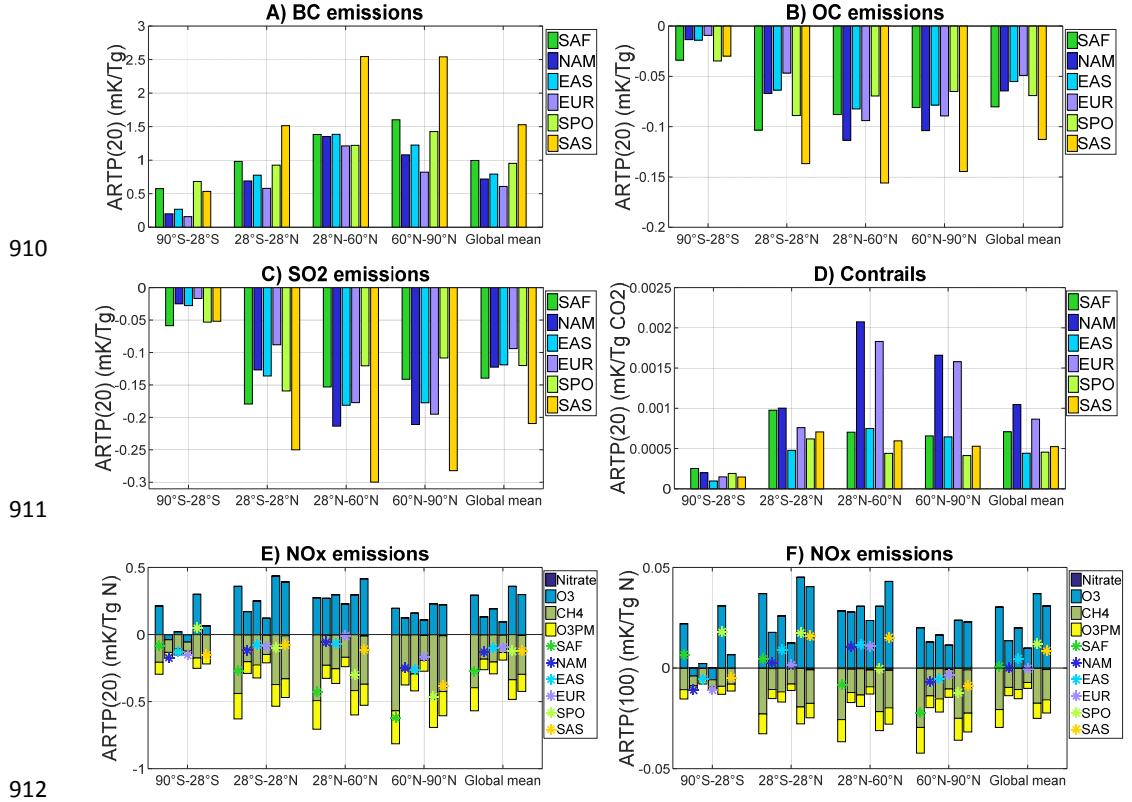

910
911
912

913 *Figure 2: ARTP(20) of aviation (A) BC, (B) OC, (C) SO_2 and (D) aviation-induced contrail-cirrus,*
914 *and (E,F) ARTP(20) and ARTP(100) of aviation NOx.*

915
916
917
918
919

Earth Syst. Dynam. Discuss., doi:10.5194/esd-2017-11, 2017
Manuscript under review for journal Earth Syst. Dynam.
Published: 7 February 2017

Earth System Dynamics
Discussions
Open Access
EGU

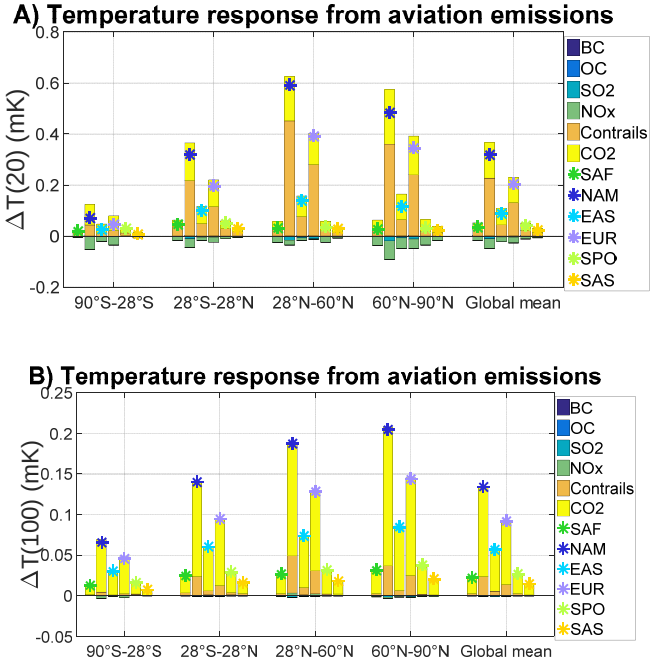

Figure 3: Regional temperature response by species and source region after A) 20 years and B) 100 years following a one-year pulse of emission from the present-day aviation sector.

Earth Syst. Dynam. Discuss., doi:10.5194/esd-2017-11, 2017
Manuscript under review for journal Earth Syst. Dynam.
Published: 7 February 2017

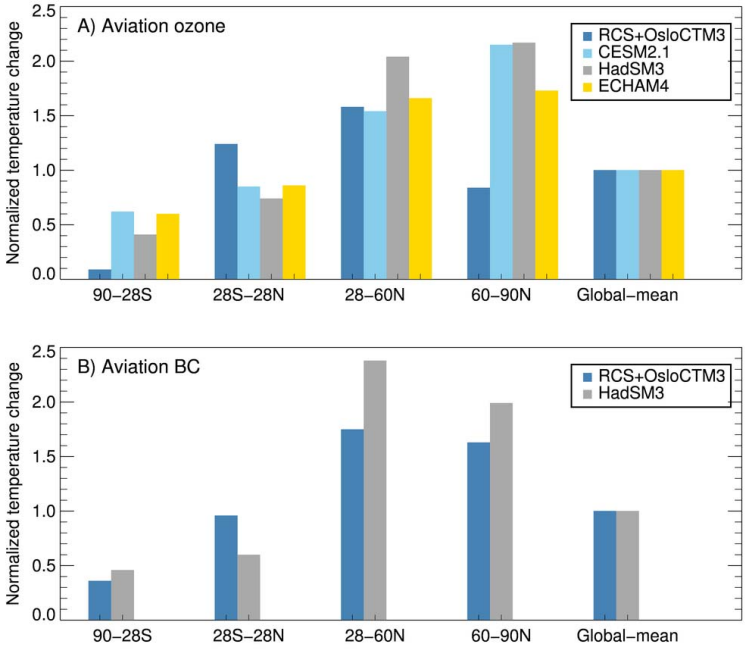

925

926 *Figure 4: A) Comparison of the regional pattern of surface temperature response to a global*
927 *aviation ozone perturbation as calculated using the regional climate sensitivities (RCS) from GISS*
928 *with RF derived from OsloCTM3 (i.e., using the ARTP concept) and simulated by HadSM3,*
929 *ECHAM4 and CESM1.2. Surface temperature response in each latitude band is normalized by the*
930 *global mean value. B) Same as A), but for BC.*

931